

Anchor-Based Adversarially Robust Zero-Shot Learning Driven by Language

Xiao Li¹ Wei Zhang¹ Yining Liu² Zhanhao Hu¹ Bo Zhang¹ Xiaolin Hu^{1,3*}

¹Department of Computer Science and Technology, BNRist, Institute for Artificial Intelligence, IDG/McGovern Institute for Brain Research, Tsinghua Laboratory of Brain and Intelligence, Tsinghua University, Beijing, China

²Harbin Institute of Technology, Weihai, China

³Chinese Institute for Brain Research (CIBR), Beijing, China

{lixiao20, zhang-w19, huzhanha17}@mails.tsinghua.edu.cn

22s030184@stu.hit.edu.cn

{dcszb, xlhu}@mail.tsinghua.edu.cn

Abstract

Deep neural networks are vulnerable to adversarial attacks. We consider adversarial defense in the case of zero-shot image classification setting, which has rarely been explored because both adversarial defense and zero-shot learning are challenging. We propose LAAT, a novel Language-driven, Anchor-based Adversarial Training strategy, to improve the adversarial robustness in a zero-shot setting. LAAT uses a text encoder to obtain fixed anchors (normalized feature embeddings) of each category, then uses these anchors to perform adversarial training. The text encoder has the property that semantically similar categories can be mapped to neighboring anchors in the feature space. By leveraging this property, LAAT can make the image model adversarially robust on novel categories without any extra examples. Experimental results show that our method achieves impressive zero-shot adversarial performance, even surpassing the previous state-of-the-art adversarially robust one-shot methods in most attacking settings. When models are trained with LAAT on large datasets like ImageNet-1K, they can have substantial zero-shot adversarial robustness across several downstream datasets.

1. Introduction

Adversarial attacks [18, 45], by adding deliberately designed perturbations to the inputs, have posed a huge threat to the application of deep neural networks (DNNs) [16, 22, 61]. In response to the threats, many techniques have been proposed to improve the adversarial robustness of DNNs. Adversarial training (AT) and its variants [33, 35, 36, 51, 56]

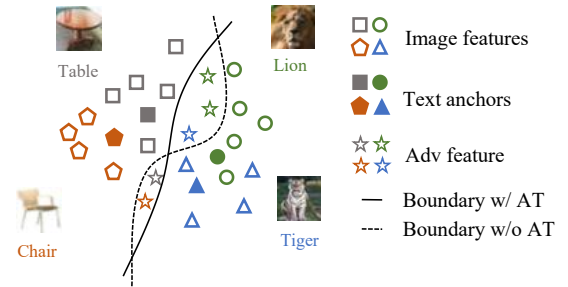


Figure 1. The illustration of zero-shot adversarial robustness of models with LAAT. Here different colors of the marks indicate different categories. When a model is adversarially trained with the text anchors of *table* and *lion* (seen categories), the model can recognize adversarial examples of the two categories (grey and green stars). Then due to the text anchors of *chair* and *tiger* (novel categories) are close to those of *table* and *lion*, respectively, the model can also classify adversarial examples of the novel categories (orange and blue stars).

are one of the most effective defense methods. However, AT is time-consuming, as several recent studies show that adversarially robust generalization needs much more data and much larger models (possibly exponential) [19, 27, 43] compared with standard generalization. The training cost of AT can be exacerbated by more data and larger model.

To improve the practical usefulness of AT, some studies propose to transfer adversarial robustness between DNN models [9, 46]. However, these methods require fine-tuning on the whole downstream datasets, still limited by the size of downstream datasets and potentially with risks such as robust overfitting [40]. Another series of works attempt to investigate adversarial robustness from a few-shot perspective [14, 42, 50], which aims to recognize novel image categories with limited data of the novel categories. AI-

*Corresponding author.

though some few-shot studies avoid fine-tuning on downstream datasets [14, 50], they need several examples of each novel category as the support set. In contrast, different from most machine learning methods, human can perform zero-shot learning easily without explicit examples of novel categories, e.g., a child can easily recognize zebra, if he/she has seen horses previously, and have the knowledge that a zebra is similar to a horse in shape and with black and white strips [37]. Moreover, human visual system is much more robust against adversarial examples [29, 60].

Motivated by the powerful capabilities of human recognition, we take a step further compared with the aforementioned few-shot adversarial defense methods. We consider adversarial defense in zero-shot setting, which aims to train an adversarially robust model that can classify objects of novel categories via transferring knowledge obtained from other seen/training categories without any examples of the novel categories. The formal definition of adversarially robust zero/few-shot classification can be found in Sec. 3. Note that both adversarial defense and zero-shot learning (ZSL) are challenging. Although there are many studies in their respective fields [25, 33, 37, 38, 51, 56], adversarial robustness under ZSL has been rarely explored before. Only two studies are related to this [55, 59]. However, both of them use the early image attribute-based ZSL methods, which have limited scalability as the attributes are hard to obtain in practice. We propose a novel Language-driven, Anchor-based Adversarial Training strategy, denoted as LAAT, to improve the scalability and practical usefulness of zero-shot adversarially robust models.

LAAT is inspired by recent advances in vision-language models [23, 38, 39]. Trained on large-scale texts pertaining to images, these models exhibit strong zero-shot capability on visual tasks without the explicit dependence on image attributes. Specially, we use the text encoder of vision-language models, e.g., CLIP [38], to obtain l_2 normalized feature embedding (named *anchor* in this paper) of the text (label name) of image categories. The text encoder has the property that semantically similar categories will be mapped to neighboring anchors in the feature space. This is called *semantic consistency*. Then we use the text anchors to adversarially supervise the image classification model. After AT, the image model will obtain adversarial robustness on seen categories and also align the image features with the text anchors. During zero-shot inference, by the semantic consistency of the text encoder on seen and novel categories, the image model can recognize novel categories with new generated anchors on novel categories. The adversarial robustness will also be kept on novel categories. Fig. 1 illustrates the idea.

However, as CLIP models are not designed for adversarial robustness, the obtained anchors are unsuitable for anchor-based AT [35, 36] directly. We analyzed the reason

in depth and found that it is mainly caused by the large cosine similarity (CoS) between anchors (see Sec. 3.1). To alleviate this, we first introduce an *expansion* algorithm remapping the original CLIP anchors into larger distances while maintaining the property of semantic consistency of original anchors. Then we relax the optimization objective of anchor-based AT methods by reintroducing the cross-entropy loss on seen categories. The overview of LAAT is shown in Fig. 2.

With these techniques, experimental results on two benchmarks showed that the models trained by LAAT achieved impressive zero-shot adversarial performance, even surpassing the previous state-of-the-art (SOTA) adversarially robust one-shot methods in most attack settings. We then trained several models with LAAT on a large dataset ImageNet-1K [41]. These models had substantial adversarial robustness across several downstream datasets in zero-shot setting like AwA2 [53] and aPY [17], without any fine-tuning. The main contributions of our work are summarized as follows:

- We propose LAAT, which can successfully train adversarially robust models in the ZSL setting. With the specially designed techniques, our ZSL method can obtain impressive zero-shot adversarial performance.
- We applied LAAT to a large dataset. The obtained models show substantial adversarial robustness across several downstream datasets, indicating that AT in the ZSL setting could be a promising way to improve the practical usefulness of AT.

To our best knowledge, this is the first work to achieve promising adversarial robustness across several datasets under the ZSL setting.

2. Related Work

Adversarial training. AT [18, 33, 51, 56] has become one of the most effective strategies to improve the adversarial robustness of models [2]. [18] first proposes AT with a single-step attack method while PGD-AT [33] improves it by introducing a multiple-step PGD attack. After that, several studies try to improve AT from various aspects [30, 35, 36, 51, 56]. One line of work focus on adjusting cross-entropy loss, which is most commonly used in classification task, to AT setting [35, 36]. [35] boosts AT by the MMC loss, a l_2 loss where there is a fixed feature vector μ_y for each category y , and the optimization object is $\|z - \mu_y\|_2^2$, where z is the output feature. [36] uses Hypersphere Embedding to boost AT. It normalizes both weights W and features z of the output layer, and proposes a loss in the form of $\cos \theta$, where θ is the angle between $\frac{W}{\|W\|_2}$ and $\frac{z}{\|z\|_2}$. Further, it replaces $\cos \theta$ with θ to be better compatible with strong adversaries. We denote the two AT methods

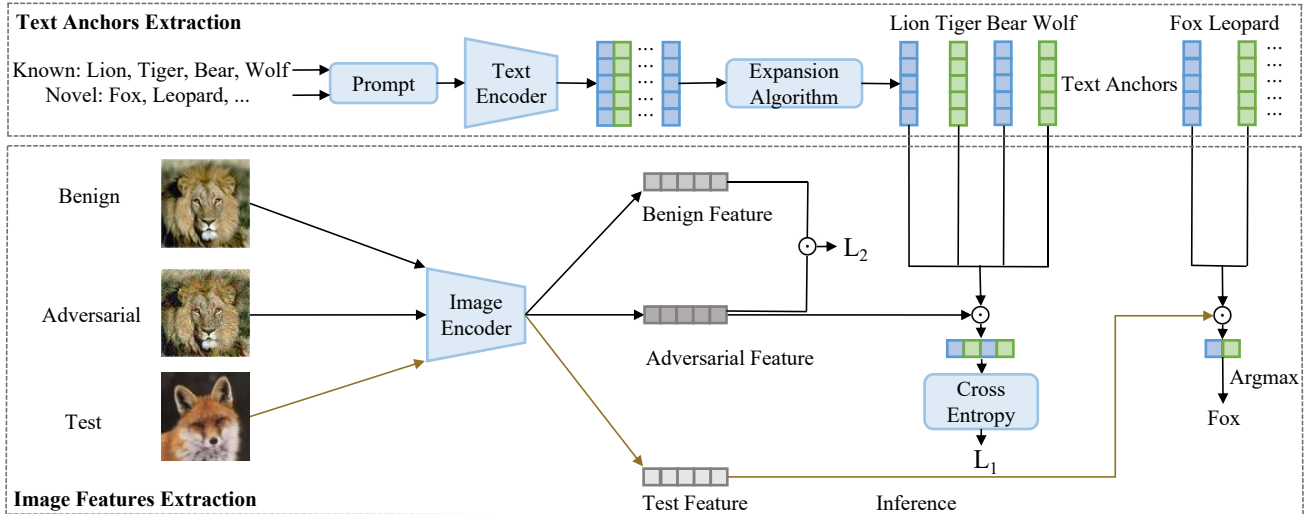


Figure 2. The pipeline of LAAT. LAAT first uses a text encoder with an expansion algorithm to obtain fixed anchors suitable for AT, then uses an image encoder to extract both benign and adversarial features. The cosine similarities between adversarial features and GT anchor are maximized by minimizing the CE loss (L_1). A smoothness loss (L_2) is applied to the adversarial and benign features directly. Only the image encoder is trainable in the illustration. \odot indicates computing the CoS. Brown arrows indicate the inference.

by anchor-based AT methods in this paper as they both have something in common with l_2 normalized feature embeddings.

Language-driven recognition. Early ZSL models exploit auxiliary information, commonly in the form of image attributes, to transfer knowledge between seen and novel categories [26, 52, 54]. Recently, language-driven recognition has caught attention in ZSL area, especially with the recent advance of large-scale pre-trained vision-language models [23, 38, 39]. Especially, Contrastive Language-Image Pre-training (CLIP) [38] demonstrated that classic recognition tasks can strongly benefit from millions of raw texts pertaining to images. CLIP uses an independent image encoder and text encoder to perform contrastive learning on 400M image-text pairs. After pre-training, natural language is used to reference visual concepts by computing the cosine similarities of text features and the visual feature, enabling zero-shot transfer of the model to downstream classification datasets. Many recent works extend the basic paradigm of CLIP to several tasks such as semantic segmentation and object detection [20, 28, 49]. CLIP model shows strong out-of-distribution robustness among several datasets such as ImageNet-Sketch [48]. However, several recent works show that the vision encoder of CLIP still lacks adversarial robustness and can be easily attacked [3, 13, 57].

Adversarially robust zero/few-shot classification. We consider adversarial robustness in the case of ZSL setting,

which has been rarely investigated. An early preprint work [59] combines AT with a ZSL, while their method relying on early attribute-based ZSL methods only gets a mild improvement and is hard to generalize without the attribute annotations. [55] evaluates the adversarial robustness of classic attribute-based zero-shot models and states that adversarial robustness for ZSL has several challenges such as the immature state of the field. Different from the lack of adversarially robust models in difficult ZSL settings, several methods investigating adversarial robustness in few-shot settings have been proposed [14, 42, 50]. We compare the performance of our method with these few-shot methods directly to comprehensively evaluate our methods.

3. LAAT

LAAT first obtains fixed text anchors from the text encoder, then uses these anchors to adversarially train an image encoder. The pipeline of LAAT is illustrated in Fig. 2. We first formulate the adversarially robust zero-shot as well as few-shot setting, then describe each module of LAAT.

Problem Formulation. Given two labeled datasets $D^{\text{tr}} = \{(\mathbf{x}_i^{\text{tr}}, y_i^{\text{tr}})\}_{i=1}^{N_{\text{tr}}}$ and $D^{\text{te}} = \{(\mathbf{x}_i^{\text{te}}, y_i^{\text{te}})\}_{i=1}^{N_{\text{te}}}$, where y^{tr} and y^{te} are disjoint category labels of images, the goal of adversarially robust ZSL is to learn a robust zero-shot classifier only on D^{tr} without querying the data on D^{te} , then it can be used to perform classification task on both benign or adversarial examples of D^{te} . Adversarially robust few-shot learning relaxes the restrictions on the access to D^{te} during training and allows to learn a robust few-shot

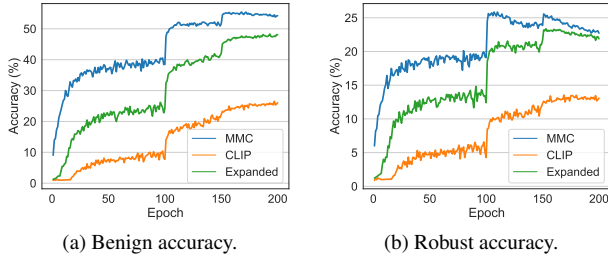


Figure 3. Learning curves of AT on CIFAR100 supervised by fixed anchors generated by MMC method, CLIP text encoder, and the expansion algorithm.

Type	RN50x4	RN50x16	ViT-B/32	ViT-B/16	ViT-L/14
Original	0.700	0.710	0.779	0.761	0.746
Expanded	0.238	0.253	0.199	0.195	0.222

Table 1. Average CoS of anchors before and after expansion algorithm from CIFAR100 categories generated by different CLIP pre-trained text encoders.

classifier with extra K examples of each category from D^{te} . This setting is also known as N_{te} -way K -shot few-shot setting. For comparison, we also name the zero-shot setting as N_{te} -way zero-shot.

3.1. Text Anchor Extraction

Given the names of N categories in the training set, we first fill them into N sentences with a fixed prompt text [6], such as ‘‘A photo of { }’’ and ‘‘This is a photo of a { }’’. After that, these sentences are encoded into N anchors $\{\mathbf{a}_i\}_{i=1}^N$ by a fixed pre-trained text encoder, where $\mathbf{a}_i \in \mathbb{R}^n$ and $\|\mathbf{a}_i\|_2 = 1$. Multiple architectures are possibly feasible if they have semantic consistency and we use the large-scale pre-trained CLIP text encoder in this work.

However, we find that if we use the original anchors from CLIP text encoder to perform anchor-base AT directly, the convergence of AT will become quite difficult. This phenomenon is universal among different CLIP text encoders and different models. For example, we adversarially trained a PreActResNet18 [21] on CIFAR100 [24] by maximizing the cosine similarities $\frac{\mathbf{z}^T \mathbf{a}_y}{\|\mathbf{z}\|_2}$ between the model output \mathbf{z} and the anchor of GT y [36] (see *Supplementary Materials* for details). The learning curves are shown in Fig. 3 (the orange curves). We can see that the accuracy with CLIP anchor increases quite slowly. Even after 200 epoch training, the accuracy is far less than that of the fixed anchor generated by MMC method [35].

To further analyze this, we also investigated the linear output layer of a PreActResNet18 with standard AT, where the learnable weights for each category can be regarded as learnable unnormalized anchors $\{\mathbf{w}_i\}_{i=1}^N$. We calculated

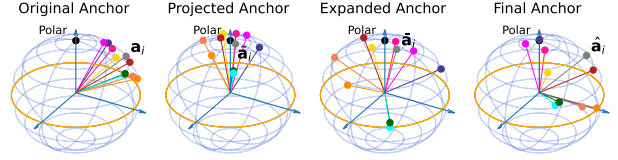


Figure 4. The pipeline of the expansion algorithm (from left to right).

the CoS of $\{\mathbf{w}_i\}$, and found that they were quite different from the CLIP anchors $\{\mathbf{a}_i\}$. The average CoS between $\{\mathbf{w}_i\}$ was quite close to 0 ($-3.8e^{-10}$). On the first row of Tab. 1 lists the average CoS of anchors from CIFAR100 [24] categories generated by different CLIP models. Note that the high CoS is irrelevant to the prompt text. Even using several random sentences from Wikipedia to encode anchors by CLIP text encoders, the average CoS was still quite large (≥ 0.67).

Although high CoS seems to have no effect on downstream tasks on benign images [20,28,49], we found that AT would be remarkably affected because higher CoS implies that the anchors are closer to the decision boundary, which could leave more room for adversarial examples [35,56]. To alleviate this phenomenon, we propose a simple yet effective expansion algorithm to enlarge the distances between different CLIP anchors (reducing the CoS).

3.2. Expansion Algorithm

The expansion algorithm aims to remap the anchors to gain lower CoS while preserving the semantic consistency between them. Large CoS means the normalized anchors $\{\mathbf{a}_i\}_{i=1}^N$ are dispersed over a cluster of the unit hyper-sphere (see Fig. 4). As we expect the remapped anchors to be also on the unit hyper-sphere, the expansion algorithm should be designed under spherical coordinates. Let us recap the transformation between n -dimensional spherical coordinate system and Cartesian coordinates. If x_i are the Cartesian coordinates, then we may compute x_1, \dots, x_n with:

$$\begin{aligned}
 x_1 &= r \cos(\phi_1); & x_2 &= r \sin(\phi_1) \cos(\phi_2); & \dots; \\
 x_{n-1} &= r \sin(\phi_1) \cdots \sin(\phi_{n-2}) \cos(\phi_{n-1}); \\
 x_n &= r \sin(\phi_1) \cdots \sin(\phi_{n-2}) \sin(\phi_{n-1}),
 \end{aligned} \tag{1}$$

where r is the distance to the axis origin, $\phi_1, \dots, \phi_{n-2}$ are angles range over $[0, \pi]$, and ϕ_{n-1} is angle range over $[0, 2\pi]$ [5]. Here ϕ_1 is the polar angle (taking the three-dimensional spherical coordinate system like longitude and latitude system as an example, the polar angle is the angle to the z axis). If the anchors are clustered around the polar, i.e., $\max_i \phi_1^i \leq \phi_0$, where ϕ_1^i denotes the polar angle of anchor \mathbf{a}_i , a natural expansion method can be evenly enlarging the polar angle ϕ_0 to $\frac{\pi}{2}$. Then the cluster can be expanded

to the whole hemisphere. Note that we cannot expand this larger than $\frac{\pi}{2}$ as anchors may be close to each other from another hemisphere, which may hurt the semantic consistency of anchors.

Thus, we first find a *center* of the clustered anchors, $\mathbf{v} := \frac{\sum_{i=1}^N \mathbf{a}_i}{\|\sum_{i=1}^N \mathbf{a}_i\|_2}$, then we calculate a rotation matrix \mathbf{R} from the center to the polar $\mathbf{p} = [1, 0, \dots, 0]^T$. The anchors can be rotated to anchors clustered around the polar: $\tilde{\mathbf{a}}_i = \mathbf{R}\mathbf{a}_i$. We then compute the largest angle θ_0 between the rotated anchors and \mathbf{p} : $\theta_0 = \arccos\{\min_{1 \leq i \leq N} \tilde{\mathbf{a}}_{i,1}\}$, where $\tilde{\mathbf{a}}_{i,1}$ denotes the first element of $\tilde{\mathbf{a}}_i$. We then obtain the polar angle of each rotated anchor: $\theta_i = \arccos \tilde{\mathbf{a}}_{i,1}$ and scale the polar angle as mentioned above: $\tilde{\theta}_i = \frac{\pi}{2} \cdot \frac{\theta_i}{\theta_0}$. According to the spherical coordinate transformation Eq. (1), the Cartesian coordinates of the expanded anchors $\bar{\mathbf{a}}_i$ are given by:

$$\begin{aligned} \bar{\mathbf{a}}_{i,1} &= \tilde{\mathbf{a}}_{i,1} \cdot \cos \tilde{\theta}_i, \\ \bar{\mathbf{a}}_{i,j} &= \tilde{\mathbf{a}}_{i,j} \cdot \frac{\sin \tilde{\theta}_i}{\sin \theta_i}, \quad j = 2, \dots, n, \end{aligned} \quad (2)$$

where $\bar{\mathbf{a}}_{i,j}$ denotes the j -th element of $\bar{\mathbf{a}}_i$. In the end, we use the inverse transformation of \mathbf{R} to map the expanded anchors $\bar{\mathbf{a}}_i$ to the original locations and obtain the final anchors: $\hat{\mathbf{a}}_i = \mathbf{R}^T \bar{\mathbf{a}}_i$. Fig. 4 shows the whole process of the expansion algorithm. As shown, the expansion algorithm can increase the distances between different anchors while maintaining the semantic consistency of the original CLIP anchors (close anchors are still close after expansion). The pseudo code of the expansion algorithm can be found in *Supplementary Materials*.

3.3. Supervision Objective

Although the CoS of anchors obtained from expansion algorithm are smaller than that from the original CLIP anchors (the second row of Tab. 1), they are still bigger than 0. Direct optimization with anchor-based AT methods, whose proposed assumption is generally that the cosine similarities are close to or less than 0, only achieves sub-optimal results (Fig. 3, MMC v.s. Expanded). Additionally, we propose to improve the anchor-based AT methods by reintroducing cross-entropy (CE) loss into the supervision objective. Assuming that the image encoder $f_{\Theta}(\cdot)$ outputs normalized features $\mathbf{z} = f_{\Theta}(\mathbf{x}) \in \mathbb{R}^n$ and $\|\mathbf{z}\|_2 = 1$, the supervision objective is given by:

$$L_1 = \mathbb{E}_{(\mathbf{x}, y)} \left[-\log \frac{\exp(f_{\Theta}(\mathbf{x} + \delta)^T \hat{\mathbf{a}}_y)}{\sum_{i=1}^N \exp(f_{\Theta}(\mathbf{x} + \delta)^T \hat{\mathbf{a}}_i)} \right], \quad (3)$$

where δ is adversarial perturbation generated by $\frac{\partial L_1}{\partial \mathbf{x}}$. This objective could make a relaxation with respect to the original anchor-based AT methods, as CE only encourages the visual feature’s cosine similarities with the GT anchor to be

larger than those with other anchors. With CE supervision, the output feature could be optimized to be far away from all anchors, but it can still be correctly classified as long as it is closest to the GT anchor. Different from previous work [28, 38] on standard training, we do not use a temperature parameter $\tau = 0.07$ to scale the CoS. We empirically find that this may be harmful under AT instead and some results are shown in *Supplementary Materials*.

3.4. Smoothness Loss

Since we prefer the adversarial robustness of the model in zero-shot transfer setting, we additionally introduce a smoothing loss, encouraging the CoS of adversarial features to be similar to the benign features of an image:

$$L_2 = \mathbb{E}_{(\mathbf{x}, y)} [-f_{\Theta}(\mathbf{x})^T f_{\Theta}(\mathbf{x} + \delta)]. \quad (4)$$

The smoothing loss is independent of the category labels of training examples. Thus, it can be expected to improve the adversarial robustness of novel categories.

Finally, the whole loss in the training stage is given by $L = L_1 + \alpha L_2$, where α is a hyper-parameter. Note that although smoothness loss has seemingly similar optimization objectives TRADES [56], it is different from TRADES in several aspects. For example, TRADES tries to minimize the classification loss on benign examples and the KL-divergence between outputs of benign and adversarial examples, and the adversarial generation is derived from the KL-divergence instead of the classification loss.

3.5. Performing Zero-Shot Recognition

When performing zero-shot recognition on novel categories, the image features of test images are generated by the image encoder, and the anchors of novel categories are generated by the text encoder and the expansion algorithm (whose internal parameters like θ_0 are pre-computed on anchors of training categories). Finally, the category corresponding to the text anchor with the maximal cosine similarities with the image feature are the prediction.

4. Experiments

4.1. Experimental Setup

Due to the lack of reliable and scalable baselines of adversarially robust methods in ZSL setting, we first applied LAAT to two popular few-shot benchmark datasets CIFAR-FS [4] and miniImageNet [47] and compared our method with several adversarially robust few-shot methods [14, 42, 50] directly. Note that zero-shot is harder than few-shot as the latter can have access to few examples of the novel categories. [42] first proposes the concept of adversarially robust few-shot classification and studies meta-learning jointly with AT. [50] further improves the performance by introducing adversarial examples during the

Method	Model	Setting	Clean	FGSM	PGD	CW	AA
AQ [42]	Conv4-512	1-shot	44.35 ± 0.49	27.94 ± 0.45	26.95 ± 0.45	25.86 ± 0.45	-
R-MAML [50]	Conv4-512	1-shot	39.22 ± 0.42	29.27 ± 0.46	27.82 ± 0.45	27.78 ± 0.45	-
GR [14]	Conv4-512	1-shot	45.27 ± 0.49	39.60 ± 0.46	38.03 ± 0.46	37.00 ± 0.46	-
LAAT	Conv4-512	zero-shot	55.59 ± 0.45	39.98 ± 0.43	38.92 ± 0.42	36.35 ± 0.42	35.54 ± 1.88
LAAT	Conv4-512	1-shot	57.92 ± 0.43	42.97 ± 0.43	41.59 ± 0.43	39.36 ± 0.43	39.77 ± 1.87
AQ [42]	ResNet12	1-shot	47.40 ± 0.52	30.37 ± 0.49	29.55 ± 0.48	28.42 ± 0.48	-
R-MAML [50]	ResNet12	1-shot	41.78 ± 0.48	34.80 ± 0.47	28.33 ± 0.46	28.86 ± 0.32	-
GR [14]	ResNet12	1-shot	48.13 ± 0.48	40.64 ± 0.45	39.29 ± 0.48	37.36 ± 0.47	-
LAAT	ResNet12	zero-shot	56.05 ± 0.43	41.42 ± 0.44	40.84 ± 0.42	38.53 ± 0.44	36.99 ± 1.91
LAAT	ResNet12	1-shot	53.75 ± 0.46	40.19 ± 0.45	39.25 ± 0.45	37.31 ± 0.45	35.24 ± 1.98

Table 2. The comparison of LAAT in 5-way zero-shot setting and previous works for 5-way 1-shot adversarially robust models on CIFAR-FS dataset. We report mean classification accuracy (%) with 95% confidence intervals on both benign and adversarial examples. We also list the performance of LAAT in 1-shot setting with image-text blended anchors (discussed in Sec. 4.3). The best results in each column are in **bold**.

Method	Model	Setting	Clean	FGSM	PGD	CW	AA
AQ [42]	Conv4-512	1-shot	34.55 ± 0.37	20.72 ± 0.30	18.87 ± 0.31	17.73 ± 0.30	-
R-MAML [50]	Conv4-512	1-shot	34.09 ± 0.36	27.36 ± 0.34	25.74 ± 0.34	26.37 ± 0.34	-
GR [14]	Conv4-512	1-shot	36.14 ± 0.45	29.23 ± 0.33	27.57 ± 0.38	26.61 ± 0.33	-
LAAT	Conv4-512	zero-shot	45.25 ± 0.37	29.41 ± 0.32	28.20 ± 0.32	28.40 ± 0.32	24.00 ± 1.36
LAAT	Conv4-512	1-shot	45.53 ± 0.26	29.92 ± 0.23	28.63 ± 0.23	28.49 ± 0.23	22.84 ± 0.96
AQ [42]	ResNet12	1-shot	41.89 ± 0.44	21.91 ± 0.31	20.53 ± 0.33	18.38 ± 0.33	-
R-MAML [50]	ResNet12	1-shot	37.52 ± 0.39	34.75 ± 0.39	27.46 ± 0.34	33.47 ± 0.34	-
GR [14]	ResNet12	1-shot	45.81 ± 0.42	36.03 ± 0.37	35.18 ± 0.40	34.53 ± 0.39	-
LAAT	ResNet12	zero-shot	53.90 ± 0.36	32.67 ± 0.33	30.22 ± 0.32	31.46 ± 0.34	25.18 ± 1.36
LAAT	ResNet12	1-shot	54.03 ± 0.26	33.07 ± 0.24	30.64 ± 0.24	31.60 ± 0.25	25.38 ± 1.02

Table 3. The comparison of LAAT and previous works for 5-way 1-shot adversarially robust models on miniImageNet dataset. The same conventions are used as in Tab. 2.

querying step in meta-training. [14] tries to learn a generalizable robust representation by the combination of several AT techniques.

We then trained several models with LAAT on ImageNet-1K [41] and evaluated them on several downstream datasets to demonstrate the scalability of our approach. These settings are discussed in Sec. 4.5. The code is submitted along with the paper and pre-trained models will be publicly available.

Dataset. CIFAR-FS [4], a variant of CIFAR100 [24], is a classification dataset containing 64 categories of training data, 16 categories of validation data, and 20 categories of test data for evaluation. It contains 600 images of 32×32 size per category. miniImageNet [47], a subset of ImageNet [41] with smaller resolution, has the same split as CIFAR-FS. It contains 600 images of 84×84 size per category. We use the same dataset splitting setting as previous few-shot works [14, 42, 50], for training and testing respectively.

Implementation details. Following [14, 42], the visual feature extraction uses two widely applied models: Conv4-512 [58] and ResNet12 [21]. We did not use Conv4-64 [14] for evaluation as it is a simple model. A learnable linear projection is applied to align the output dimension of image backbones and the length of text anchors.

For a fair comparison, the training recipe strictly followed the previous few-shot work [14]. We performed AT by generating adversarial examples via PGD method with maximum adversarial perturbation $\epsilon = 8/255$ in l_∞ -norm bound, with $T = 7$ iterative steps with the step size as $2/255$. Unless otherwise stated, we used the CLIP ViT-B/16 text encoder and the prompt text was set as “This is a photo of a { }”. α was simply set to 1 during training.

4.2. Compared with Few-Shot Methods

We report the robustness of our method against common white-box adversarial attacks, including FGSM [18],

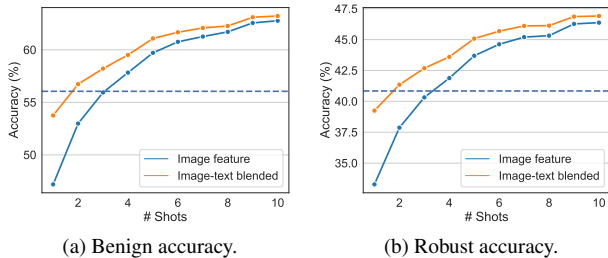


Figure 5. Classification accuracy on both benign and adversarial examples in 5-way few-shot setting on CIFAR-FS, with image feature anchors or with image-text blended anchors. The dashed line denotes 5-way zero-shot accuracy.

PGD [33] with 20 iterative steps and step size 2 (denoted as PGD-20 in the following text), CW [7] (optimized by PGD for 30 steps with step size 0.8), and AutoAttack (AA) [11], an effective attack used to assess adversarial robustness. The maximal adversarial perturbation is set to be $\epsilon = 8/255$ in l_∞ setting. We performed experiments under the usual 5-way one/zero-shot setting [14, 42, 50]. The experimental results are reported from 2000 randomly sampled 5-way tasks. Tab. 2 and 3 presents the experimental results on CIFAR-FS [4] and miniImageNet [47] respectively.

The results on two benchmarks show that LAAT under zero-shot setting is competitive with several methods under few-shot setting. Except for the result on miniImageNet with ResNet12 as the backbone, the adversarial robustness of LAAT models even surpassed those from the previous SOTA adversarially robust one-shot method [14]. The benign accuracy of our method is also significantly better than all of the three few-shot methods by a large margin.

4.3. Extending LAAT to Few-Shot Setting

Our zero-shot models supervised by LAAT can be naturally extended to few-shot setting and the robustness can be further improved. Given the images of novel categories as the support set, we can follow previous few-shot SOTA GR [14] and use the prototype-based metric learning [44] to build image feature-based anchors, i.e., in the K -shot case, the image anchor \mathbf{v}_y for a novel category y can be computed as $\mathbf{v}_y = \text{Norm}_2\{\sum_{i=1}^K f_\Theta(\mathbf{x}_i)\}$, where \mathbf{x}_i denotes the images of y in the support set and $\text{Norm}_2\{\cdot\}$ denotes the l_2 normalization. We can also weight the original text anchor \mathbf{a}_y from the text encoder and the image feature from the support set to build an image-text blended anchor for y : $\hat{\mathbf{a}}_y^* = \text{Norm}_2\{\beta \cdot \mathbf{a}_y + \sum_{i=1}^K f_\Theta(\mathbf{x}_i)\}$. Here the text anchor can be regarded as the *prior knowledge* of y . We set $\beta = 2$ for all experiments.

Tab. 2 and 3 show the results of different models with image-text blended anchors in one-shot setting. In most cases (except ResNet12 on CIFAR-FS), 1-shot performance of LAAT can further surpass the zero-shot performance.

Objective	Clean	Robust
l_2	43.3 ± 0.5	29.0 ± 0.4
θ	45.2 ± 0.5	29.7 ± 0.4
$\cos \theta$	45.8 ± 0.5	30.0 ± 0.4

Table 4. Classification accuracy (%) of ResNet12 supervised by the original CLIP anchors with different optimization objectives.

$\cos(\theta)$	SP	CE	SM	Clean	Robust	Clean	Robust
✓				25.25	13.54	45.8 ± 0.5	30.0 ± 0.4
✓	✓			45.71	23.37	45.7 ± 0.5	32.5 ± 0.4
✓	✓	✓		50.49	25.58	59.4 ± 0.5	38.9 ± 0.4
✓	✓	✓	✓	49.38	27.12	56.1 ± 0.4	40.8 ± 0.4

Table 5. Classification accuracy (%) of PreActResNet18 on seen categories in CIFAR-100 test set in standard evaluation setting (left) and ResNet12 on novel categories in CIFAR-FS in 5-way zero-shot setting (right) under different ablation experiments.

Fig. 5 further shows the results of a ResNet-12 model with two different anchors $\hat{\mathbf{a}}^*$ and \mathbf{v} in K -shot settings. We can see that the text anchor used to perform zero-shot recognition can also boost the performance in various K -shot setting, especially when the support set is small.

4.4. Ablation Study

Unless otherwise specified, the ablations are performed on CIFAR-FS with the ResNet12, in the 5-way zero-shot setting. And the robust accuracy is evaluated by PGD-20.

Effectiveness of each design. In Fig. 3 we have shown that if the model is supervised by CoS between the original CLIP anchors and the output feature, it is difficult to converge under adversarial training in the standard recognition task. Here we further validate this in the zero-shot task. We used several different optimization objectives proposed by the anchor-based AT methods, including the CoS [36], the angle [36], and the l_2 distance [35] between the output feature and anchors, denoted as $\cos \theta$, θ , and l_2 , respectively. The results in Tab. 4 show that all these optimization objectives fail if using the original CLIP anchors directly in the 5-way zero-shot setting (note that random guessing in this setting can obtain 20% accuracy).

We then conducted ablation study to show the effectiveness of each design in LAAT: the expansion algorithm, the reintroduced CE loss, and the smoothness loss, denoted as SP, CE, and SM, respectively. Here except the 5-way zero-shot setting, we also performed ablation study in the setting of Fig. 3 to investigate the performance of each design on seen categories, as the robustness on both seen and novel categories is the key to the success of our following generalized ZSL setting [8] (Sec. 4.5). The results in Tab. 5 show

AT Method	Hyper-Parameter	Clean	Robust
TRADES [56]	$1/\lambda = 1$	50.0 ± 0.5	16.6 ± 0.4
	$1/\lambda = 6$	53.3 ± 0.5	24.2 ± 0.4
AWP [51]	$\gamma = 1e^{-3}$	59.0 ± 0.5	40.1 ± 0.4
	$\gamma = 1e^{-2}$	61.2 ± 0.5	41.0 ± 0.5
SM (Ours)	$\alpha = 0.5$	57.5 ± 0.5	40.9 ± 0.4
	$\alpha = 2.0$	58.9 ± 0.5	42.2 ± 0.4
SM + AWP	$\gamma = 1e^{-2}, \alpha = 0.5$	58.6 ± 0.5	42.8 ± 0.4
	$\gamma = 1e^{-2}, \alpha = 2.0$	56.4 ± 0.5	42.7 ± 0.4

Table 6. Classification accuracy (%) of ResNet-12 on CIFAR-FS under different AT methods. Here all experiments are performed based on expanded anchors with CE supervision.

Text Encoder	Embed-Dim	Clean	Robust
RN50x4	640	54.5 ± 0.4	38.9 ± 0.4
RN50x16	768	57.3 ± 0.4	38.9 ± 0.4
ViT-B/32	512	53.2 ± 0.4	38.2 ± 0.4
ViT-B/16	512	56.1 ± 0.4	40.8 ± 0.4
ViT-L/14	768	55.7 ± 0.4	39.5 ± 0.5

Table 7. Classification accuracy (%) of ResNet-12 supervised by the full LAAT with different CLIP text encoders on CIFAR-FS. Embed-Dim denotes the dimension of the text anchors.

that all of these designs are helpful to improve the adversarial robustness. With the smoothness loss (see SM), the accuracy on benign examples slightly drops. This can be due to the setting of hyper-parameter α . We will discuss this next.

As stated before, CE could make a relaxation compared with the original anchor-based methods. To validate this, we computed the average CoS between GT anchors and the output visual features of the two models trained on CIFAR-FS in Tab. 5: $\cos \theta + \text{SP}$ and $\cos \theta + \text{SP} + \text{CE}$. With CE loss, the visual feature’s CoS with GT anchors dropped from 0.455 to 0.205 in average, while the accuracies on both benign and adversarial examples improved a lot. These results support our conjecture that some examples not quite close to the GT anchor can still be classified correctly with CE supervision.

Compared with other AT methods. To further show the effectiveness of LAAT, especially the smoothness loss, we compared the smoothness loss with TRADES [56] and AWP [51]. Recently AWP is a popular and effective AT method in avoiding adversarial overfitting in standard AT setting. Here all experiments are performed based on expanded anchors with CE supervision. The results are shown in Tab. 6, together with the most important hyper-parameter of each method. Among these methods, TRADES per-

Dataset	Category	Model	Clean	Robust
CIFAR100	100	ConvNeXt-T	26.15	6.38
		XCiT-S12/16	26.43	6.88
		ViT-B/16	30.75	7.11
aPY	32	ConvNeXt-T	62.62	35.75
		XCiT-S12/16	61.22	32.75
		ViT-B/16	63.75	34.97
AwA2	50	ConvNeXt-T	55.83	25.92
		XCiT-S12/16	52.37	24.00
		ViT-B/16	59.04	26.21
COCO Objects	80	ConvNeXt-T	47.30	21.96
		XCiT-S12/16	45.61	19.46
		ViT-B/16	48.59	20.61

Table 8. Classification accuracy (%) of models trained on ImageNet-1K with LAAT on several downstream datasets. The number of categories per dataset is reported. The accuracy is reported by sampling 100 examples per category on all splits of the datasets. The robustness is evaluated by PGD-20 ($\epsilon = 8/255$).

formed the worst while our smoothness loss achieved comparable (or even better) robust accuracy with AWP. To investigate whether our method can be combined with AWP, we set γ in AWP to be $1e^{-2}$ according to the results, and incorporated AWP into the pipeline of LAAT. The results at the bottom of Tab. 6 show that LAAT with AWP can further boost the adversarial robustness in zero-shot setting.

Different text encoders. Arbitrary text encoders are feasible in principle for LAAT if they have semantic consistency. We show the influence of using different CLIP text encoders in Tab. 7. Note that the text encoders of different CLIP models have the same transformer-based architecture that purely operates on the text. The different names in Tab. 7 are the names of the paired image encoders during CLIP pre-training. We studied the relationship between the distances of different CLIP models’ anchors and CIFAR100 super-categories. The results in *Supplementary Materials* show that semantic consistency of the text encoder is one of the keys to zero-shot adversarial robustness.

4.5. Pre-Training on ImageNet

To further demonstrate the scalability and flexibility of the LAAT framework, we then performed experiments in the generalized zero-shot learning setting [8], which is a more pragmatic version of ZSL. This setting requires recognizing examples from both seen and novel categories.

We pre-trained several modern models with LAAT on the large dataset ImageNet-1K [41]. The training basically followed the recipe proposed by [12], which was the Top-1 AT recipe on RobustBench [10] at the submission time. The only difference is that we used the expanded CLIP anchors

to supervise the models. We trained three competitive visual models: ConvNeXt-T [32], XcIT-S12/16 [1], and ViT-B/16 [15], from scratch for 110 epochs under $\epsilon = 8/255$. We test these models on several downstream datasets including CIFAR100 [24], AwA2 [53], aPY [17], and COCO Objects [31]. AwA2 and aPY are two popular datasets in ZSL setting. COCO Objects are images extracted from the bounding box annotations of MS COCO [31]. Note that all of these datasets include several novel categories that have never appeared in ImageNet-1K, e.g., *statue* and *ass* in aPY, *blue whale* and *dolphin* in AwA2.

The models were evaluated on N -way classification setting, where N is the number of categories in each dataset. All images on downstream datasets are resized to 224×224 in inference. Tab. 8 shows the zero-shot results on downstream datasets without any fine-tuning. All these models with LAAT performed promising zero-shot robustness on aPY, AwA2, and COCO Objects. Note that they did not perform well on CIFAR100 and this could be caused by the original small resolution of CIFAR100 (32×32) [12, 34].

5. Conclusion and Discussion

In this work, we propose a novel adversarial training strategy LAAT for robust image classification in a zero-shot setting, inspired by recent vision-language models. Extensive experiments demonstrate that our method has strong adversarial robustness across several zero-shot settings. We hope our work could encourage more researchers to investigate the robustness in zero-shot setting and robust pre-trained large models based on this setting.

Limitation. Limited by the data and computation resources, we cannot perform adversarial training on large-scale image-text pairs directly like CLIP. We believe it can be a promising way to achieve both adversarial and out-of-distribution robustness. And with this setting, the problem brought by the anchors obtained from recent CLIP text encoders might be naturally addressed.

Acknowledgements. This work was supported in part by the National Natural Science Foundation of China (Nos. U19B2034, 62061136001, 61836014) and the Tsinghua-Toyota Joint Research Fund.

References

- [1] Alaaeldin Ali, Hugo Touvron, Mathilde Caron, Piotr Bojanowski, Matthijs Douze, Armand Joulin, Ivan Laptev, Natalia Neverova, Gabriel Synnaeve, Jakob Verbeek, and Hervé Jégou. Xcit: Cross-covariance image transformers. In *Adv. Neural Inform. Process. Syst. (NeurIPS)*, pages 20014–20027, 2021. 9
- [2] Anish Athalye, Nicholas Carlini, and David A. Wagner. Obfuscated gradients give a false sense of security: Circumventing defenses to adversarial examples. In *Int. Conf. Mach. Learn. (ICML)*, volume 80, pages 274–283, 2018. 2
- [3] Yuanhao Ban and Yinpeng Dong. Pre-trained adversarial perturbations. *Adv. Neural Inform. Process. Syst. (NeurIPS)*, 2022. 3
- [4] Luca Bertinetto, João F. Henriques, Philip H. S. Torr, and Andrea Vedaldi. Meta-learning with differentiable closed-form solvers. In *Int. Conf. Learn. Represent. (ICLR)*, 2019. 5, 6, 7
- [5] LE Blumenson. A derivation of n-dimensional spherical coordinates. *The American Mathematical Monthly*, 67(1):63–66, 1960. 4
- [6] Tom B. Brown, Benjamin Mann, Nick Ryder, et al. Language models are few-shot learners. In *Adv. Neural Inform. Process. Syst. (NeurIPS)*, 2020. 4
- [7] Nicholas Carlini and David A. Wagner. Towards evaluating the robustness of neural networks. In *IEEE Symposium on Security and Privacy, SP*, pages 39–57, 2017. 7
- [8] Wei-Lun Chao, Soravit Changpinyo, Boqing Gong, and Fei Sha. An empirical study and analysis of generalized zero-shot learning for object recognition in the wild. In *Eur. Conf. Comput. Vis. (ECCV)*, volume 9906, pages 52–68, 2016. 7, 8
- [9] Tianlong Chen, Sijia Liu, Shiyu Chang, Yu Cheng, Lisa Amini, and Zhangyang Wang. Adversarial robustness: From self-supervised pre-training to fine-tuning. In *IEEE Conf. Comput. Vis. Pattern Recog. (CVPR)*, pages 696–705, 2020. 1
- [10] Francesco Croce, Maksym Andriushchenko, Vikash Sehswag, Edoardo Debenedetti, Nicolas Flammarion, Mung Chiang, Prateek Mittal, and Matthias Hein. Robustbench: a standardized adversarial robustness benchmark. In *NeurIPS Datasets and Benchmarks*, 2021. 8
- [11] Francesco Croce and Matthias Hein. Reliable evaluation of adversarial robustness with an ensemble of diverse parameter-free attacks. In *Int. Conf. Mach. Learn. (ICML)*, volume 119, pages 2206–2216, 2020. 7
- [12] Edoardo Debenedetti, Vikash Sehswag, and Prateek Mittal. A light recipe to train robust vision transformers. *arXiv preprint arXiv:2209.07399*, 2022. 8, 9
- [13] Benjamin Devillers, Bhavin Choksi, Romain Bielawski, and Rufin VanRullen. Does language help generalization in vision models? In *CoNLL*, pages 171–182, 2021. 3
- [14] Junhao Dong, Yuan Wang, Jianhuang Lai, and Xiaohua Xie. Improving adversarially robust few-shot image classification with generalizable representations. In *IEEE Conf. Comput. Vis. Pattern Recog. (CVPR)*, pages 9015–9024. IEEE, 2022. 1, 2, 3, 5, 6, 7
- [15] Alexey Dosovitskiy, Lucas Beyer, Alexander Kolesnikov, et al. An image is worth 16x16 words: Transformers for image recognition at scale. In *Int. Conf. Learn. Represent. (ICLR)*, 2021. 9
- [16] Kevin Eykholt, Ivan Evtimov, Earlene Fernandes, Bo Li, Amir Rahmati, Chaowei Xiao, Atul Prakash, Tadayoshi Kohno, and Dawn Song. Robust physical-world attacks on

- deep learning visual classification. In *IEEE Conf. Comput. Vis. Pattern Recog. (CVPR)*, pages 1625–1634, 2018. **1**
- [17] Ali Farhadi, Ian Endres, Derek Hoiem, and David A. Forsyth. Describing objects by their attributes. In *IEEE Conf. Comput. Vis. Pattern Recog. (CVPR)*, pages 1778–1785, 2009. **2, 9**
- [18] Ian J. Goodfellow, Jonathon Shlens, and Christian Szegedy. Explaining and harnessing adversarial examples. In *Int. Conf. Learn. Represent. (ICLR)*, 2015. **1, 2, 6**
- [19] Sven Gowal, Sylvestre-Alvise Rebuffi, Olivia Wiles, Florian Stimberg, Dan Andrei Calian, and Timothy A. Mann. Improving robustness using generated data. In *Adv. Neural Inform. Process. Syst. (NeurIPS)*, pages 4218–4233, 2021. **1**
- [20] Xiuye Gu, Tsung-Yi Lin, Weicheng Kuo, and Yin Cui. Zero-shot detection via vision and language knowledge distillation. In *Int. Conf. Learn. Represent. (ICLR)*, 2021. **3, 4**
- [21] Kaiming He, Xiangyu Zhang, Shaoqing Ren, and Jian Sun. Deep residual learning for image recognition. In *IEEE Conf. Comput. Vis. Pattern Recog. (CVPR)*, pages 770–778, 2016. **4, 6**
- [22] Zhanhao Hu, Siyuan Huang, Xiaopei Zhu, Fuchun Sun, Bo Zhang, and Xiaolin Hu. Adversarial texture for fooling person detectors in the physical world. In *IEEE Conf. Comput. Vis. Pattern Recog. (CVPR)*, pages 13297–13306, 2022. **1**
- [23] Chao Jia, Yinfei Yang, Ye Xia, Yi-Ting Chen, Zarana Parekh, Hieu Pham, Quoc V. Le, Yun-Hsuan Sung, Zhen Li, and Tom Duerig. Scaling up visual and vision-language representation learning with noisy text supervision. In *Int. Conf. Mach. Learn. (ICML)*, volume 139, pages 4904–4916, 2021. **2, 3**
- [24] Alex Krizhevsky, Geoffrey Hinton, et al. Learning multiple layers of features from tiny images. 2009. **4, 6, 9**
- [25] Christoph H. Lampert, Hannes Nickisch, and Stefan Harmeling. Attribute-based classification for zero-shot visual object categorization. *IEEE Trans. Pattern Anal. Mach. Intell. (TPAMI)*, 36(3):453–465, 2014. **2**
- [26] Christoph H. Lampert, Hannes Nickisch, and Stefan Harmeling. Attribute-based classification for zero-shot visual object categorization. *IEEE Trans. Pattern Anal. Mach. Intell. (TPAMI)*, 36(3):453–465, 2014. **3**
- [27] Binghui Li, Jikai Jin, Han Zhong, John E. Hopcroft, and Liwei Wang. Why robust generalization in deep learning is difficult: Perspective of expressive power. *Adv. Neural Inform. Process. Syst. (NeurIPS)*, 2022. **1**
- [28] Boyi Li, Kilian Q. Weinberger, Serge J. Belongie, Vladlen Koltun, and René Ranftl. Language-driven semantic segmentation. In *Int. Conf. Learn. Represent. (ICLR)*, 2022. **3, 4, 5**
- [29] Xiao Li, Jianmin Li, Ting Dai, Jie Shi, Jun Zhu, and Xiaolin Hu. Rethinking natural adversarial examples for classification models. *arXiv preprint arXiv:2102.11731*, 2021. **2**
- [30] Xiao Li, Ziqi Wang, Bo Zhang, Fuchun Sun, and Xiaolin Hu. Recognizing object by components with human prior knowledge enhances adversarial robustness of deep neural networks. *IEEE Trans. Pattern Anal. Mach. Intell. (TPAMI)*, 2023. **2**
- [31] Tsung-Yi Lin, Michael Maire, Serge J. Belongie, James Hays, Pietro Perona, Deva Ramanan, Piotr Dollár, and C. Lawrence Zitnick. Microsoft COCO: common objects in context. In *Eur. Conf. Comput. Vis. (ECCV)*, volume 8693, pages 740–755, 2014. **9**
- [32] Zhuang Liu, Hanzi Mao, Chao-Yuan Wu, Christoph Feichtenhofer, Trevor Darrell, and Saining Xie. A convnet for the 2020s. In *IEEE Conf. Comput. Vis. Pattern Recog. (CVPR)*, pages 11966–11976, 2022. **9**
- [33] Aleksander Madry, Aleksandar Makelov, Ludwig Schmidt, Dimitris Tsipras, and Adrian Vladu. Towards deep learning models resistant to adversarial attacks. In *Int. Conf. Learn. Represent. (ICLR)*, 2018. **1, 2, 7**
- [34] Yichuan Mo, Dongxian Wu, Yifei Wang, Yiwen Guo, and Yisen Wang. When adversarial training meets vision transformers: Recipes from training to architecture. *Adv. Neural Inform. Process. Syst. (NeurIPS)*, 2022. **9**
- [35] Tianyu Pang, Kun Xu, Yinpeng Dong, Chao Du, Ning Chen, and Jun Zhu. Rethinking softmax cross-entropy loss for adversarial robustness. In *Int. Conf. Learn. Represent. (ICLR)*, 2020. **1, 2, 4, 7**
- [36] Tianyu Pang, Xiao Yang, Yinpeng Dong, Taufik Xu, Jun Zhu, and Hang Su. Boosting adversarial training with hypersphere embedding. In *Adv. Neural Inform. Process. Syst. (NeurIPS)*, 2020. **1, 2, 4, 7**
- [37] Farhad Pourpanah, Moloud Abdar, Yuxuan Luo, Xinlei Zhou, Ran Wang, Chee Peng Lim, and Xi-Zhao Wang. A review of generalized zero-shot learning methods. *IEEE Trans. Pattern Anal. Mach. Intell. (TPAMI)*, 2022. **2**
- [38] Alec Radford, Jong Wook Kim, Chris Hallacy, Aditya Ramesh, Gabriel Goh, Sandhini Agarwal, Girish Sastry, et al. Learning transferable visual models from natural language supervision. In *Int. Conf. Mach. Learn. (ICML)*, volume 139, pages 8748–8763, 2021. **2, 3, 5**
- [39] Aditya Ramesh, Mikhail Pavlov, Gabriel Goh, Scott Gray, Chelsea Voss, Alec Radford, Mark Chen, and Ilya Sutskever. Zero-shot text-to-image generation. In *Int. Conf. Mach. Learn. (ICML)*, volume 139 of *Proceedings of Machine Learning Research*, pages 8821–8831, 2021. **2, 3**
- [40] Leslie Rice, Eric Wong, and J. Zico Kolter. Overfitting in adversarially robust deep learning. In *Int. Conf. Mach. Learn. (ICML)*, volume 119, pages 8093–8104, 2020. **1**
- [41] Olga Russakovsky, Jia Deng, Hao Su, Jonathan Krause, Sanjeev Satheesh, Sean Ma, Zhiheng Huang, Andrej Karpathy, Aditya Khosla, Michael S. Bernstein, Alexander C. Berg, and Li Fei-Fei. Imagenet large scale visual recognition challenge. *Int. J. Comput. Vis. (IJCV)*, 115(3):211–252, 2015. **2, 6, 8**
- [42] Hadi Salman, Andrew Ilyas, Logan Engstrom, Ashish Kapoor, and Aleksander Madry. Do adversarially robust imagenet models transfer better? In *Adv. Neural Inform. Process. Syst. (NeurIPS)*, 2020. **1, 3, 5, 6, 7**
- [43] Ludwig Schmidt, Shibani Santurkar, Dimitris Tsipras, Kunal Talwar, and Aleksander Madry. Adversarially robust generalization requires more data. In *Adv. Neural Inform. Process. Syst. (NeurIPS)*, pages 5019–5031, 2018. **1**
- [44] Jake Snell, Kevin Swersky, and Richard S. Zemel. Prototypical networks for few-shot learning. In *Adv. Neural Inform. Process. Syst. (NeurIPS)*, pages 4077–4087, 2017. **7**

- [45] Christian Szegedy, Wojciech Zaremba, Ilya Sutskever, Joan Bruna, Dumitru Erhan, Ian J. Goodfellow, and Rob Fergus. Intriguing properties of neural networks. In *Int. Conf. Learn. Represent. (ICLR)*, 2014. 1
- [46] Pratik Vaishnavi, Kevin Eykholt, and Amir Rahmati. Transferring adversarial robustness through robust representation matching. In *USENIX Security Symposium*, pages 2083–2098, 2022. 1
- [47] Oriol Vinyals, Charles Blundell, Tim Lillicrap, Koray Kavukcuoglu, and Daan Wierstra. Matching networks for one shot learning. In *Adv. Neural Inform. Process. Syst. (NeurIPS)*, pages 3630–3638, 2016. 5, 6, 7
- [48] Haohan Wang, Songwei Ge, Zachary C. Lipton, and Eric P. Xing. Learning robust global representations by penalizing local predictive power. In *Adv. Neural Inform. Process. Syst. (NeurIPS)*, pages 10506–10518, 2019. 3
- [49] Mengmeng Wang, Jiazheng Xing, and Yong Liu. Actionclip: A new paradigm for video action recognition. *arXiv preprint arXiv:2109.08472*, 2021. 3, 4
- [50] Ren Wang, Kaidi Xu, Sijia Liu, Pin-Yu Chen, Tsui-Wei Weng, Chuang Gan, and Meng Wang. On fast adversarial robustness adaptation in model-agnostic meta-learning. In *Int. Conf. Learn. Represent. (ICLR)*, 2021. 1, 2, 3, 5, 6, 7
- [51] Dongxian Wu, Shu-Tao Xia, and Yisen Wang. Adversarial weight perturbation helps robust generalization. In *Adv. Neural Inform. Process. Syst. (NeurIPS)*, 2020. 1, 2, 8
- [52] Yongqin Xian, Zeynep Akata, Gaurav Sharma, Quynh Nguyen, Matthias Hein, and Bernt Schiele. Latent embeddings for zero-shot classification. In *IEEE Conf. Comput. Vis. Pattern Recog. (CVPR)*, pages 69–77, 2016. 3
- [53] Yongqin Xian, Christoph H. Lampert, Bernt Schiele, and Zeynep Akata. Zero-shot learning - A comprehensive evaluation of the good, the bad and the ugly. *IEEE Trans. Pattern Anal. Mach. Intell. (TPAMI)*, 41(9):2251–2265, 2019. 2, 9
- [54] Yunlong Yu, Zhong Ji, Yanwei Fu, Jichang Guo, Yanwei Pang, and Zhongfei (Mark) Zhang. Stacked semantics-guided attention model for fine-grained zero-shot learning. In *Adv. Neural Inform. Process. Syst. (NeurIPS)*, pages 5998–6007, 2018. 3
- [55] Mehmet Kerim Yucel, Ramazan Gokberk Cinbis, and Pinar Duygulu. How robust are discriminatively trained zero-shot learning models? *Image Vis. Comput.*, 119:104392, 2022. 2, 3
- [56] Hongyang Zhang, Yaodong Yu, Jiantao Jiao, Eric P. Xing, Laurent El Ghaoui, and Michael I. Jordan. Theoretically principled trade-off between robustness and accuracy. In *Int. Conf. Mach. Learn. (ICML)*, volume 97, pages 7472–7482, 2019. 1, 2, 4, 5, 8
- [57] Jiaming Zhang, Qi Yi, and Jitao Sang. Towards adversarial attack on vision-language pre-training models. In *ACM Int. Conf. Multimedia*, pages 5005–5013, 2022. 3
- [58] Manli Zhang, Jianhong Zhang, Zhiwu Lu, Tao Xiang, Mingyu Ding, and Songfang Huang. IEPT: instance-level and episode-level pretext tasks for few-shot learning. In *Int. Conf. Learn. Represent. (ICLR)*, 2021. 6
- [59] Xingxing Zhang, Shupeng Gui, Zhenfeng Zhu, Yao Zhao, and Ji Liu. ATZSL: defensive zero-shot recognition in the presence of adversaries. *arXiv preprint arXiv:1910.10994*, 2019. 2, 3
- [60] Zhenglong Zhou and Chaz Firestone. Humans can decipher adversarial images. *Nature communications*, 10(1):1–9, 2019. 2
- [61] Xiaopei Zhu, Xiao Li, Jianmin Li, Zheyao Wang, and Xiaolin Hu. Fooling thermal infrared pedestrian detectors in real world using small bulbs. In *AAAI*, pages 3616–3624, 2021. 1